



OPEN ACCESS

EDITED BY

Yu-Fei Wu,
RMIT University, Australia

REVIEWED BY

Dilan Robert,
RMIT University, Australia
Jiaqing Wang,
Nanjing Forestry University, China

*CORRESPONDENCE

Nan Chen,
✉ ChenNanRIOH@hotmail.com
Yongyan Yu,
✉ 535165839@qq.com

[†]These authors share first authorship

RECEIVED 29 July 2023

ACCEPTED 01 November 2023

PUBLISHED 14 November 2023

CITATION

Yu Y, Chen N, Li L and Wang J (2023),
Assessment of chlorine resistance in
concrete in the tidal range and splash
zone of a torrid marine region.
Front. Mater. 10:1269124.
doi: 10.3389/fmats.2023.1269124

COPYRIGHT

© 2023 Yu, Chen, Li and Wang. This is an
open-access article distributed under the
terms of the [Creative Commons
Attribution License \(CC BY\)](https://creativecommons.org/licenses/by/4.0/). The use,
distribution or reproduction in other
forums is permitted, provided the original
author(s) and the copyright owner(s) are
credited and that the original publication
in this journal is cited, in accordance with
accepted academic practice. No use,
distribution or reproduction is permitted
which does not comply with these terms.

Assessment of chlorine resistance in concrete in the tidal range and splash zone of a torrid marine region

Yongyan Yu^{1*†}, Nan Chen^{1*†}, Lihui Li¹ and Jian Wang²

¹Research Institute of Highway Ministry of Transport, Beijing, China, ²China Highway Engineering Consulting Corporation, Beijing, China

Based on China's long-term goals for 2035, numerous projects are expected to be constructed in torrid marine regions, with increased chloride ion erosion, particularly in tidal and splash zones. To improve chlorine resistance performance, in this work, we proposed a method to assess the chlorine resistance of concrete in the tidal range and splash zones of a torrid marine region. To ensure consistency in assessment, an enhanced Fuzzy analytic hierarchy process (F-AHP) method was applied. 1) The factors that affected the chloride resistance of concrete in the tidal range and splash zones in torrid marine regions were theoretically analyzed. 2) The factors were classified into concrete material properties, concrete structure location, and marine organism impact, which have been insufficiently mentioned in previous chlorine resistance assessments and other protective measures. The weight of factors was calculated in an enhanced F-AHP method to ensure the consistency of judgment matrices from expert investigations. Membership functions were obtained based on engineering requirements, standards, and specifications to enhance their applicability to engineering. 3) The assessment was then applied to the marine concrete engineering of the Xiapu Bridge in Hainan Province, China, with apparent characteristics of a torrid marine environment. The methods for improving the chlorine resistance of concrete were subsequently proposed.

KEYWORDS

assessment, chlorine resistance, tidal range and splash zone, torrid marine region, enhanced F-AHP

1 Introduction

China's long-term goals for 2035 include promoting the Belt and Road initiative as well as constructing the New Western Land-sea Corridor. The Hainan Province in China and some southeast Asian countries in the Belt and Road and New Western Land-sea Corridor have a torrid marine climate, and these regions experience high solar radiation intensity, resulting in a warm climate. In these environments, the damage and deterioration of concrete are caused by significantly higher intense corrosive ions than in inland areas. Reinforced concrete structures are generally designed for a lifetime of 50–100 years; these structures will deteriorate after 20–30 years when in contact with chloride ions (Bastidas-Arteaga et al., 2010); (Poupard et al., 2006); (Mehta, 1997). Consequently, chlorides have long been considered the main driver of corrosion in concrete structures in marine environments (Richardson, 2002); (Melchers and Chaves, 2021). Due to their dry-wet alternating environment, the chloride penetration of concrete will significantly accelerate in the splash and tidal zones in torrid marine regions.

Due to the effect of chloride ions on concrete, evaluating the chloride ion resistance of concrete in the tidal range and splash zone is critical in torrid marine regions.

At this stage, the evaluation of concrete durability has mainly considered the contribution of mineral admixtures or admixtures in concrete durability tests. However, in the evaluation process, additional consideration should be given to factors such as the environmental characteristics of the concrete structure, the impact of marine organisms on durability, and design and construction. Al-Hashem et al. (Al-Hashem et al., 2022) investigated the effect of metakaolin (M.K.), Habib et al. (Habib et al., 2022) studied the effect of bentonite, Mathews et al. (Mathews et al., 2023) used industrial by-products, Yuan et al. (Yuan et al., 2021) applied electric arc furnace oxidizing slag (EAS), Yoon et al. (Yoon and Lee, 2020) tested fly ash (FA), silica fume (SF), and natural zeolite as water repellency, Lee et al. (Lee and Lee, 2020); (Lee et al., 2020) mixed locally produced ground granulated blast-furnace slag (GGBS), Stratoura et al. (Stratoura et al., 2023) mixed perlite and rice husk ash as fine aggregates, and Prithiviraj et al. (Prithiviraj et al., 2022) used alccofine as an additive material to evaluate the durability of concrete.

Studies have evaluated the chloride resistance of concrete according to different influencing factors on chloride ions. However, research must consider the environmental characteristics of torrid marine regions, especially in tidal and splash zones, which are more susceptible to corrosion. Amin et al. (Amin et al., 2022) used a genetic programming approach to investigate rapid chloride ion penetration (RCP), while Imounga et al. (Imounga et al., 2020) assessed chloride ingress into reinforced concrete by Bayesian networks, and Mukhti et al. (Mukhti et al., 2023) evaluated early concrete damage caused by chloride-induced steel corrosion using a deep learning approach based on RNN for ultrasonic pulse waves. Huang et al. (Huang et al., 2023) predicted the chloride permeability coefficient based on improved machine-learning techniques, and Li et al. (Li et al., 2021) used the posable set theory to analyze and calculate the weights of factors acting on durability, which were combined with a fuzzy evaluation method. Chen et al. (Chen et al., 2015) evaluated the durability of in-service concrete using an improved three-scale hierarchical analysis method and fuzzy topology theory, while Cai et al. (Cai et al., 2019) evaluated the durability of concrete in a chloride ion attack environment using a fuzzy integrated evaluation method. Luhar et al. (Luhar et al., 2021) used a variety of indices to evaluate concrete durability.

According to the literature, significant research progress has been made in assessing the chlorine resistance of concrete. However, existing research has focused more on evaluating mineral admixtures to improve the chloride resistance of concrete, rather than evaluating the chloride resistance of concrete under multiple factors. Some assessments have used machine learning or statistic analysis, with significant information related to durability. However, research must consider the environmental characteristics of torrid marine regions, with significantly greater corrosion than inland areas. Therefore, considering the lack of existing research and the need for chlorine resistance performance, it is necessary to establish a concrete chlorine resistance evaluation system for tidal and splash zones in hot sea tide environments under multiple factors that affect conditions.

This study provides a new approach for assessing the chloride resistance of concrete in tidal range and splash zones in torrid

marine regions, in which multiple types of influencing factors were considered instead of single elements like in traditional assessments. This included the impact of marine organisms on concrete and differences in chloride resistance in tidal and splash zones, which have not been extensively investigated in previous chlorine resistance assessments. An enhanced F-AHP method was used in this study to ensure the consistency of judgment matrixes from expert investigations. First, the factors affecting chloride resistance were theoretically analyzed. Second, the factors were classified into concrete material properties, concrete structure location, and marine organism impact. These have not been mentioned in previous chlorine resistance assessments and other protective measures. The weight of each factor was calculated using an enhanced F-AHP method, which could reduce the probability of calibration inconsistency directly from expert surveys and from indirect calculations, ensuring the consistency of judgment matrixes from expert investigations. Membership functions were obtained based on engineering requirements, standards, and specifications related to the project to enhance its engineering applicability. Third, the assessment was applied to marine concrete engineering in the tidal range and splash zones in Xiapu Bridge in Hainan Province, China, with apparent characteristics of a torrid marine environment. According to the project and assessment factors, the methods for improving the chlorine resistance of concrete were subsequently proposed.

2 Methodology

In this study, an enhanced F-AHP method was used to evaluate the chloride ion resistance of concrete in the tidal range and splash zone in torrid marine regions. This improved method was based on the traditional AHP method to improve consistency certification during questionnaires in weight calculation.

This evaluation considered various factors including concrete properties, location, and marine organism impact on concrete and construction.

2.1 Evaluation process

The proposed evaluation process was carried out as follows.

(1) Analysis of the influencing factors

The material properties contributing to concrete's chloride ion response were theoretically analyzed. The impact of marine organisms on the chloride ion content in concrete in the torrid oceanic region was considered, and the biological species that were found to survive in the tidal range and splash zone were summarized. External protection, design, and construction factors that contributed to durability were also studied.

(2) Obtaining factors based on the questionnaire survey

Factors were screened through expert surveys, and the participants included researchers and experts from research units, universities, and construction units.

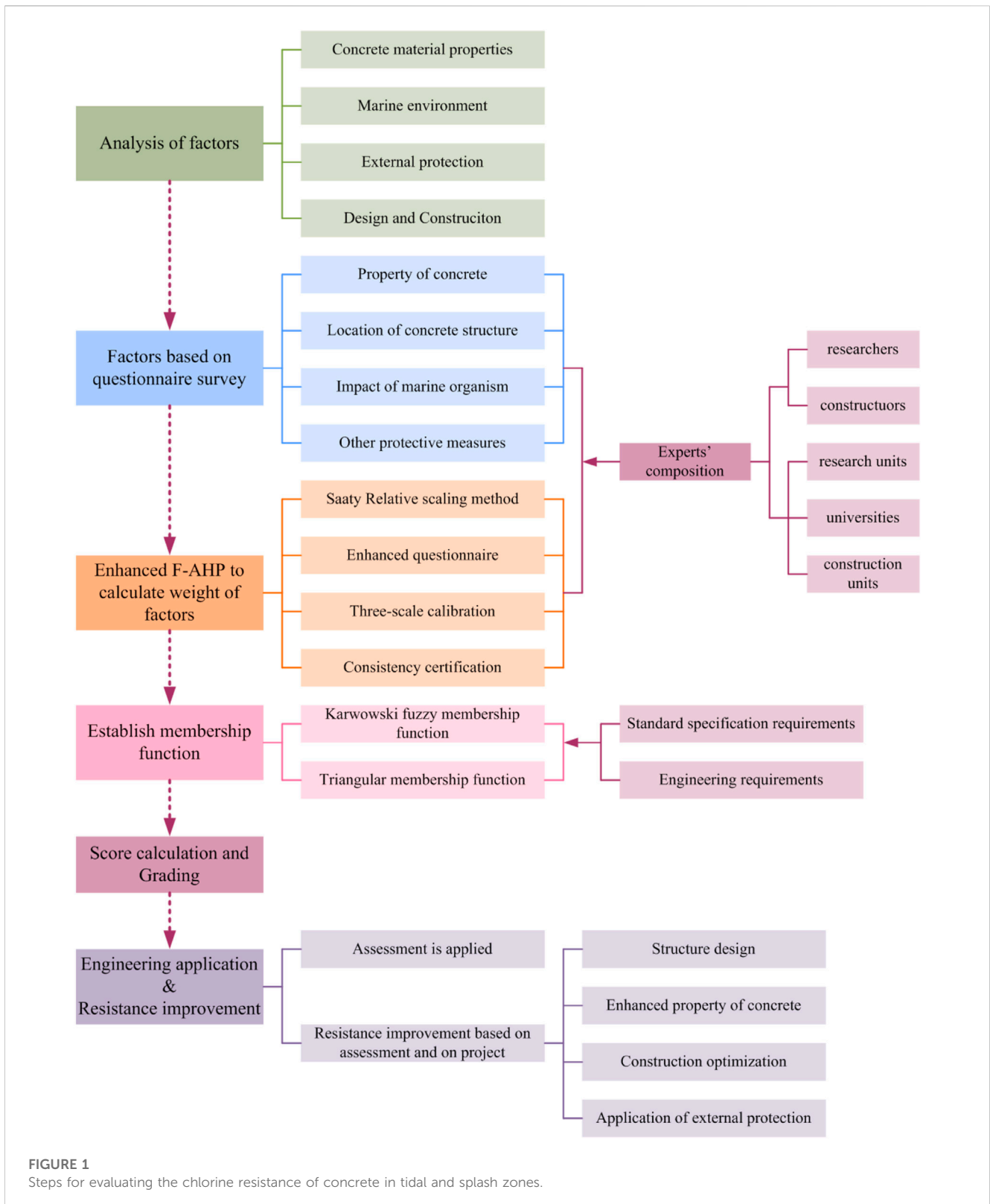


FIGURE 1
Steps for evaluating the chlorine resistance of concrete in tidal and splash zones.

The factors in the questionnaire survey were based on concrete property, the positional relationship between concrete structure and organisms, differences in resistance to chloride ions between tidal range and splash zone, substantial surface protection, structural design, and construction performance.

(3) Enhanced F-AHP used to establish assessment

Enhanced questionnaires and weight calculations were used to improve consistency certification in this study. The enhanced F-AHP method could reduce the probability of inconsistency of calibration

TABLE 1 Saaty relative scaling method.

Calibration	Meaning
1	The former had the same importance as the latter
3	The former was slightly more important than the latter
5	The former was significantly more important than the latter
7	The former was intensively more important than the latter
9	The former was extremely more important than the latter
2, 4, 6, 8	Represent the median value of the adjacent judgment
a_{ji}	If the ratio of element i and element j was a_{ij} , the ratio of element j to element i was $a_{ji} = 1/a_{ij}$

directly from expert surveys and from indirect estimates. The feature vector was obtained from the weight of each factor, and the membership function was built based on standard specifications and engineering requirements. After multiplying the feature vector by the membership function, the final evaluation grade was determined according to the maximum membership degree principle.

The standard specification and engineering requirements were associatively considered in determining the membership function factors to increase engineering applicability. The assessment would be suspended if the value of influencing factors exceeded standard specifications and engineering requirements.

(4) Engineering application and chlorine resistance improvements

An assessment was conducted in this study, where chlorine resistance improvement was proposed based on the evaluation and case. The modification contained structure design, enhanced concrete property, construction optimization, and application of external protection.

The evaluation process is shown in Figure 1.

2.2 Enhanced F-AHP method

F-AHP, which combined the advantages of the analytic hierarchy process (AHP) with the fuzzy set, has been widely used in assessment.

AHP, proposed by Saaty et al. (Saaty, 1980) (Saaty, 2001), can divide factors into several levels, establishing hierarchical structure models according to the intrinsic relationship among factors, setting judgment matrices through comparison of characteristics, and deciding the relationship of factor importance.

Zadeh et al. (Zadeh, 1965) proposed the fuzzy set theory, which can be combined with the AHP method in the assessment of various fields.

The main steps of establishing enhanced F-AHP included identifying factors, establishing a judgment matrix, establishing membership functions, fuzzy estimation, and assessment results.

2.2.1 Identifying factors

The factors of chlorine resistance of concrete in the tidal range and splash zone in the torrid marine region could be obtained based on theoretical analysis and questionnaire survey.

2.2.2 Establishing a judgment matrix to calculate the weight

2.2.2.1 Judgment matrix using the traditional F-AHP method

According to the consistency certification, the weight of each factor could be calculated using the Saaty method for traditional AHP evaluation.

The Saaty method determined the relative importance of factor 1 to factor I , and Saaty could divide the factor relative importance of the target into 1–9 levels, describing them with a_{ij} , as shown in Table 1.

The characteristics of a_{ij} were as follows:

$$\begin{cases} a_{ij} > 0 \\ a_{ii} = 1 \\ a_{ij} = 1/a_{ji} \end{cases}$$

The judgment matrix was established by formula 1, based on calibration results

$$A = \begin{bmatrix} a_{11} & a_{12} & \dots & a_{1n} \\ a_{21} & a_{22} & \dots & a_{2n} \\ \dots & \dots & \dots & \dots \\ a_{n1} & a_{n2} & \dots & a_{nn} \end{bmatrix} \tag{1}$$

2.2.2.2 Enhanced questionnaire and weight calculation

According to expert investigation, inconsistency in traditional methods may occur. For example, after the calibration of a_{1i} and a_{1j} , a_{ij} could be calculated, and the meaning of a_{ij} from expert investigation may be consistent with the intention of a_{ij} from the calculation. Consequently, an enhanced questionnaire and weight calculation were used to build an improved F-AHP method to avoid potential inconsistency.

This study used a new questionnaire to establish consistent judgment matrices proposed by Yu et al. (Yu et al., 2022). In this new questionnaire, the three-scale method designed by Yu et al. and the Saaty scale method were used to comprehensively determine the relative importance of factors for these criteria. The process of enhanced questionnaire and weight calculation was as follows.

- (a) The relative importance of factor 1 to factor i was determined by the Saaty scale method, which was used to determine the relative importance of factor 1 to factor i , based on an investigation by experts. Furthermore, the calibration of a_{1i} ($i = 1-n$) was obtained.
- (b) The relative importance of factor i ($i \neq 1$) to factor j ($j \neq 1$) was determined by the three-scale method.

The relative importance of factor i ($i \neq 1$) to factor j ($j \neq 1$) was compared qualitatively by experts. The qualitative analysis included the following: same important, more important, and less important.

- (c) Consistency conformation

The values of “same important,” “more important,” and “less important” in the three-scale method were assigned as a_{ij-3s} , and the assignment of a_{ij-3s} consisted of a numerical interval.

The evaluation in a three-scale method is qualitative. The calibration of a_{ij-3s} is shown in Table 2.

TABLE 2 Relative value in three scaling methods.

Calibration a_{ij-3s}	Meaning
1/3-3	The former had the same importance as the latter
4-9	The former was more important than the latter
¼-1/9	The former was less important than the latter

The pairwise comparison of factors, calculated by assessing a_{1i} and a_{1j} using the Saaty method, was assigned as a_{ij-Ss} .

The consistency was also satisfied if the value of a_{ij-Ss} was in the numerical interval of a_{ij-3s} , with a_{ij} taking the closest data in the Saaty calibration. A further questionnaire was needed if the value of a_{ij-Ss} exceeded the numerical break of a_{ij-3s} .

The new questionnaire could satisfy the consistency if the value of a_{ij-Ss} consisted of the trend of a_{ij-3s} because a_{ij-Ss} was obtained from the logical computation of a_{1i} and a_{1j} , evaluated from expert quantitative calibration using the Saaty method. Thus, a_{ij-3s} , as a numerical interval qualitative calibration, reflected the relationship between factor i and factor j . When a_{ij-Ss} consisted of the trend of a_{ij-3s} , quantitative and qualitative feedback was compatible.

The new questionnaire could satisfy the consistency if the value of a_{ij-Ss} consisted of the trend of a_{ij-3s} because a_{ij-Ss} was obtained from the logical computation of a_{1i} and a_{1j} , evaluated from expert quantitative calibration in the Saaty method. Thus, a_{ij-3s} , as a numerical interval qualitative calibration, reflected the relationship between factor i and factor j . When a_{ij-Ss} consisted of the trend of a_{ij-3s} , quantitative and qualitative feedback was compatible.

For example, in the Saaty scale method from the questionnaire, the expert calibrated $a_{14} = 7$ and $a_{15} = 3$, and the Saaty scale method calculated the pairwise comparison of factor a_{ij-Ss} with $a_{45-Ss} = 3/7$. The expert filled out a questionnaire to compare the relative importance of factor 4 to factor 5 qualitatively. If the feedback was listed as same important, the calibration of a_{45-3s} was 1/3-3, according to Table 2. The value of $a_{45-Ss} = 3/7$ was in the numerical interval of $a_{45-3s} = 1/3-3$, and the consistency was satisfied. Furthermore, a_{45} took the closest data in the Saaty calibration; thus, $a_{45} = 1/2$.

If the feedback of relative importance between factor 4 to factor 5 was more important, the calibration of a_{45-3s} was 4-9, according to Table 2. If the value of $a_{45-Ss} = 3/7$ was outside the numerical interval of $a_{45-3s} = 4-9$, the consistency was not satisfied, and a further questionnaire was needed.

2.2.3 Consistency certification

The judgment matrix provided by each expert could be obtained based on the questionnaire results, where the enhanced questionnaire and weight calculation in Section 2.2.2 guaranteed the consistency of the judgment matrix. However, the final judgment matrix, composed of the matrix formed by the expert research results, could certify its consistency.

Multiplying the elements of each line in the judgment matrix A, as shown in Formula 1, gave the following equation:

$$M_i = \prod_{j=1}^n a_{ij}, \quad i = 1, 2, \dots, n \tag{2}$$

The result of the multiplication of elements in each line was to the n th power

$$\overline{W}_i = \sqrt[n]{M_i} \tag{3}$$

The weight vector W_i was obtained by normalizing the vector.

$$W_i = \frac{\overline{W}_i}{\sum_{j=1}^n \overline{W}_j} \quad i = 1, 2, \dots, n \tag{4}$$

where $W = \{W_1, W_2, \dots, W_n\}^T$ is the obtained feature vector.

We calculated the maximum characteristic square root of the judgment matrix as follows:

$$\lambda_{\max} = \sum_{i=1}^n \frac{(AW_i)}{nW_i} \tag{5}$$

We subsequently calculated the index CI to measure the degree of inconsistency of judgment matrix A

$$CI = \frac{\lambda_{\max} - n}{n-1} \tag{6}$$

When the average random consistency ratio was $CR < 0.1$, the consistency of ranking results was acceptable

$$CR = CI/RI \tag{7}$$

According to the order of matrix A, we could determine the value of the average random consistency index RI in Table 3. The first-order and second-order matrices were always entirely consistent, making it unnecessary to test CR .

2.2.4 Establishing membership function

The I-type function was used when utilizing language to describe factors in establishing the membership function. The Karwowski fuzzy membership function was used to calculate the assignment values in this study, as shown in Table 4.

The triangular membership function, denoted as (a,b,c), employed fuzzy numbers (Lyu et al., 2020) and is used when a numerical value could describe factors. In this stage, the triangular membership function has been widely used in the fuzzy-AHP mode when evaluating real-life problems. The function is given by

$$\mu_{A(x)} = \begin{cases} 0 & x < a \\ \frac{x-a}{b-a} & a \leq x < b \\ \frac{c-x}{c-b} & b \leq x < c \\ 0 & c \leq x \end{cases} \tag{8}$$

2.2.5 Fuzzy estimation

The fuzzy estimation was obtained by multiplying the feature vector through the membership function, as follows:

TABLE 3 Average random consistency indicator *RI* (L et al., 2013).

Order of A	3	4	5	6	7	8	9	10	11	12	13	14	15
<i>RI</i>	0.52	0.9	1.12	1.26	1.36	1.41	1.46	1.49	1.52	1.54	1.56	1.58	1.59

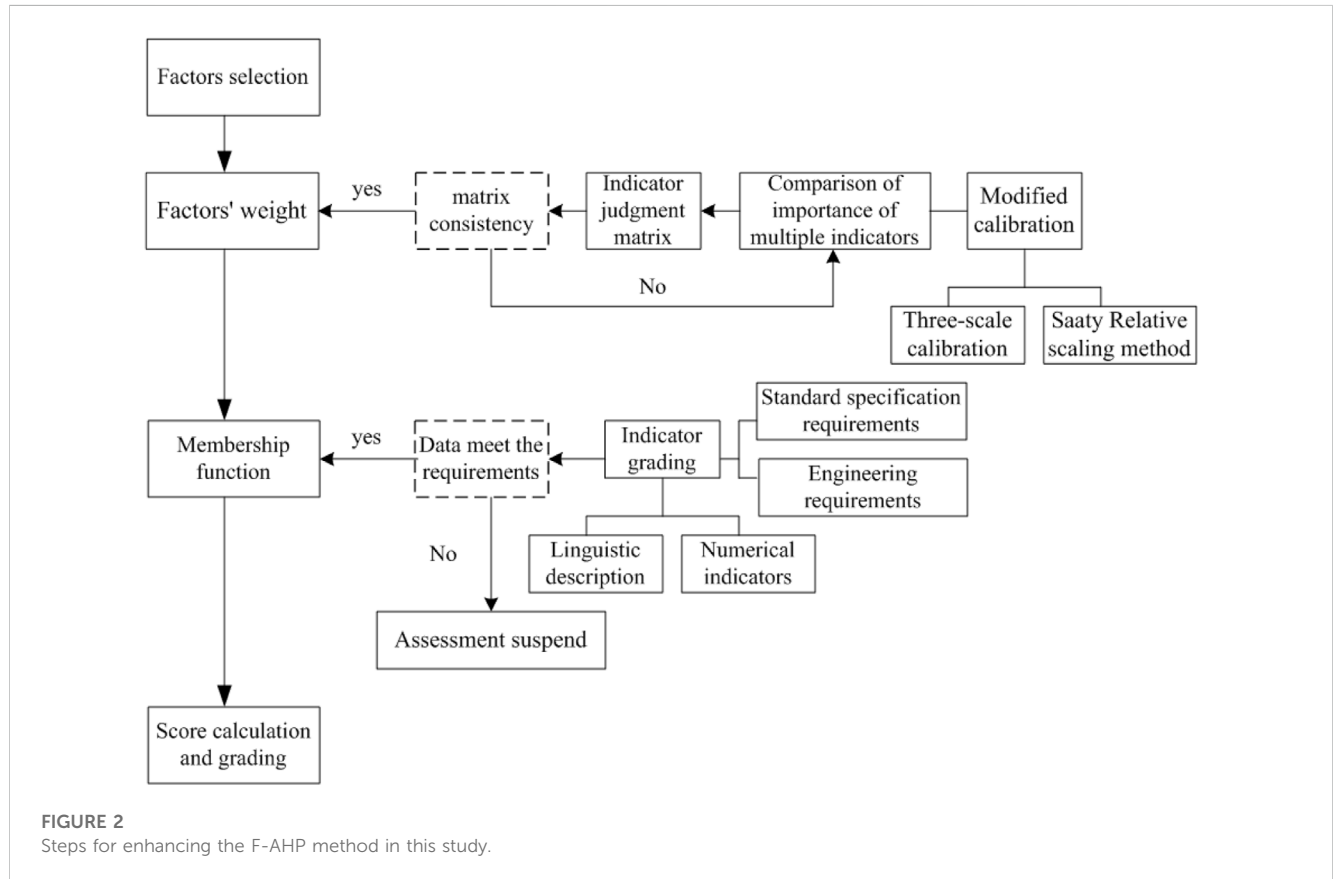


FIGURE 2 Steps for enhancing the F-AHP method in this study.

TABLE 4 Karwowski fuzzy membership functions (Karwowski and Mital, 1986).

Fuzzy language variable	Membership function						
High	0	0	0.1	0.3	0.7	0.9	1
Medium	0	0.2	0.7	1	0.7	0.2	0
Low	1	0.9	0.7	0.3	0.1	0	0
Unknown	1	1	1	1	1	1	1
Undefined	0	0	0	0	0	0	0
More or less high	0	0	0.3	0.5	0.85	0.95	1
Very high	0	0	0	0.1	0.5	0.8	1
Likely	0	0.1	0.5	0.7	0.9	1	1
Unlikely	1	1	0.9	0.8	0.5	0	0
Not Likely	1	1	0.5	0.3	0.1	0.1	0

The feature vector of the factor layer was obtained from Formula 4. The factor value, which could be described by numerical value, was obtained using formula 8. The factor value, which could not be defined by a numerical value, is given in Table 4 based on fuzzy language.

2.2.6 Results of assessment

In this study, evaluation results were processed by the maximum value method, with the evaluation index corresponding to the maximum membership degree taken as the evaluation result. According to the fuzzy estimation results, the chloride resistance was divided into three levels, namely, excellent, sound, and average.

The steps for the enhanced F-AHP method in this study are shown in Figure 2.

3 Factors affecting the chloride resistance of concrete

Due to its inherent pores and micro-cracks, concrete contains natural channels that allow for the diffusion of chloride ions. Therefore, factors that affect the pore structure and interface area of concrete will also affect its resistance to chloride resistance.

$$B = W_i \cdot R_i = \{W_1, W_2, \dots, W_n\} \cdot \begin{Bmatrix} R_{11}, & R_{12}, \dots, & R_{1n} \\ R_{21}, & R_{21}, \dots, & R_{2n} \\ \dots & & \\ R_{n1}, & R_{n2}, \dots, & R_{nm} \end{Bmatrix} \quad (9)$$

The factors that generally affect the chlorine resistance of concrete in torrid marine regions include concrete material properties, marine environment, external protection, design, and construction.

3.1 Concrete material properties

3.1.1 The effect of concrete material ratio on chlorine resistance

Concrete components with good compactness can effectively prevent or slow down corrosion. The compactness of concrete will be related to the water-to-cement ratio, mineral admixtures, nanomaterials, aggregate properties, and the amount of water reducer addition.

Concrete compactness will also increase with a decrease in water-to-cement ratio, with more substantial chloride resistance. Due to the volcanic ash, micro aggregate, and adsorption effects of mineral admixtures such as FA, mineral powder, and SF, the concrete pores can be filled, improving the structure of the concrete interface transition zone. As a result, mineral admixtures can reduce the porosity of concrete and improve its chloride resistance. The use of hydrophobic agents can also reduce the permeability of concrete and improve its resistance to chloride ion corrosion, while the filling and nucleation effects of nanomaterials in concrete can improve its pore structure and enhance its chlorine resistance. Commonly used nanomaterials include SiO₂, nano TiO₂, nano Al₂O₃, and nano CaCO₃. Sufficient sand content can also reduce the porosity of concrete, improve the structure of the concrete interfacial transition zone, and improve the resistance of concrete to chloride ion corrosion. Therefore, the larger the particle size of the coarse aggregate, the easier for concrete to develop expansion cracks, resulting in more severe corrosion. Water-reducing agents can also effectively improve the compactness of concrete.

3.1.2 Control of chloride ions in raw materials

The chloride ion content of concrete raw materials must be controlled. According to the standard specifications in China, chloride ions in cement production should not exceed 0.5%. This control mainly involves preventing cement from affecting the quality of the concrete. In marine sand, many chloride ions will stay on the sand surface and increase the chloride ion content, due to high chloride ion content in seawater. The content of chloride ions in groundwater, recycled water, washing water for cement company equipment, and seawater also needs to be considered, to determine whether the water can be used.

3.1.3 Chloride resistance test of concrete

The chlorine resistance of concrete can be assessed using various experimental methods, and multiple relevant standards and specifications in China have used testing methods and indicators to determine the chloride resistance of concrete.

The evaluation methods for chloride ion penetration resistance of concrete in China have mainly focused on the rapid chloride ion detection method (RCM method) and electric flux method. The main techniques for inspecting and evaluating chloride ion penetration in concrete worldwide include the natural diffusion method, electrical quantity method, and electrical resistance (conductivity) method.

3.2 Marine environment

3.2.1 Marine conditions

Hainan Province and its surrounding areas belong to a tropical marine climate area, with an annual average temperature of 23°C–25°C, yearly light exposure of 1750–2,650 h, light intensity of 50%–60%, and intense sunlight radiation. Hainan Province, located on the western coast, has an average salt content of seawater of 3.34%, with a maximum of 3.50%. This is higher than the seawater salinity of 2.10%–3.60% for the sea area location of the Sulamadu Cross Sea Bridge in Indonesia, which belongs to the same tropical marine region. Therefore, Hainan Province is considered one of the most corrosive environments in China.

Hainan Province, located in the South China Sea, has characteristics of high temperature, high humidity, high salt, and high sunlight. Corrosive ions in seawater, ocean tides, salt mist, and sunlight, combined with wind and waves, can cause various types of damage to concrete materials and structures. The damage and deterioration rate of local concrete materials caused by intense corrosive ions and harsh environments are significantly higher than inland areas.

3.2.2 Corrosion of concrete in marine environments

The ocean is considered one of the most naturally corrosive environments, and the marine corrosive environment can be vertically divided into five regions: the maritime atmospheric zone, splash zone, tidal range zone, and underwater zone (including the fully submerged zone of seawater and the seabed soil zone).

The splash and tidal zones consist of dry, wet, alternating environments caused by water level changes. Compared to austere dry or wet environments, the rate of chloride ions in seawater entering unsaturated concrete under alternating dry and wet environments will be significantly enhanced.

The environmental conditions and corrosion characteristics are shown in [Table 5](#).

Concrete structures are most susceptible to corrosion in the splash and tidal range zones, with the concrete structure often in an alternating dry and wet state in these zones, providing convenient conditions for chloride ion diffusion, infiltration, and capillary adsorption. This environment also provides sufficient oxygen and water, accelerating steel corrosion. Therefore, corrosion prevention of concrete structures in ocean splash zones and tidal ranges is essential.

3.2.3 Impact of marine organisms on chloride resistance

3.2.3.1 Organisms in different regions

The lower layer of the tidal range area covers oysters; however, the upper layer of the tidal range area contains fewer oysters, with most of the site occupied by barnacles. The time to contact water in the splash zone will be shorter than that in the tidal area; thus, a visible biofilm will rarely form on concrete components in the splash zone.

TABLE 5 Environmental conditions and corrosion characteristics in the splash and tidal zones.

Splash zone	Environmental condition	Humid and adequately oxygenated, without marine fouling
Tidal zone	Corrosion characteristics	Area with the most severe corrosion, with anti-corrosion coatings most susceptible to damage
	Environmental condition	Alternating dry-wet environment, usually with sufficient oxygen
	Corrosion characteristics	Relatively severe corrosion

3.2.3.2 Impact of marine organisms on chloride resistance

The long-term adhesion of barnacles and oysters can affect concrete surface coatings. Biological attachment to the concrete structure surfaces can cause the concrete surface to detach, and animals such as barnacles and oysters release mucilage and natural acids in metabolites on the concrete surface through suction cups. This action corrodes the concrete material and destroys the protective layer on the reinforced concrete shell, which reacts with $\text{Ca}(\text{OH})_2$ in the concrete to generate gypsum, producing ettringite through a series of reactions and leading to expansion and cracking of the concrete (Wang J. and Yan, 2009).

Marine animals can also strengthen concrete, mainly due to solid adhesive biological adhesives formed by organisms such as oysters and shells. Biological adhesives form a dense microstructure adhesive layer after adhering to the concrete structure, which can improve the ability of concrete to resist Cl^- corrosion.

Floating algae can significantly impact concrete structures, where the higher the porosity of concrete, the more favorable the environment for algae (Rong et al., 2012). Algae can absorb metal ions in concrete through metabolism, taking in minerals such as calcium aluminate sulfate, orthorhombic calcium zeolite, sodium hydroxide crystal, as well as raw materials, and absorb calcium, silicon, magnesium, and other elements, leading to concrete degradation (Wang J. C. and Yan, 2009); (Yennawar et al., 1999). This can subsequently lead to the corrosion and destruction of concrete structures.

Microorganisms have both corrosive and protective effects on concrete. Microorganisms mainly corrode and destroy concrete structures through metabolism, which can be divided into physical and chemical processes. The physical action involves microorganism damage not only to the surface of concrete but also to the internal concrete structure through concrete pores. As a result, concrete structures in tidal areas covered with microorganisms on the surface are often loose and porous. Chemical reactions consist of two aspects, namely, the direct metabolism of biological acids and the reduction of sulfate in concrete to generate H_2S .

3.3 External protection

To improve resistance to chloride ion corrosion, many studies have assessed the resistance of coated concrete to chloride salt corrosion by applying organic protective coatings on the concrete surface via electrochemical protection, or through concrete surface coatings.

Organic film-forming coatings form a film layer on the concrete surface, preventing the ingress of external substances, with this protective layer completely separating the substrate from external

substances, providing good protection. Therefore, these films have high property requirements and generally include water resistance and corrosion resistance, along with film-forming coatings exhibiting impermeable properties.

Sacrificial anode protection has been commonly used in electrochemical protection methods. Cast iron or active metal can serve as the anode, while steel bars in concrete serve as the cathode, and direct current can be applied to reduce the oxidation reaction near the steel bars. Protecting the cathode steel bars can be achieved through the primary battery reaction, thus reducing the corrosion of steel bars caused by a decrease in the chloride resistance of concrete.

The concrete surface coating can be used to effectively prevent harmful media such as Cl^- , CO_2 , and water from entering the interior of the concrete, thereby achieving chlorine resistance. Protective materials such as polyurethane/polyurea (SPUA), organosilicon hydrophobic penetrating agents, and anti-corrosion coatings have been used for this purpose.

3.4 Design and construction

3.4.1 Concrete cover

The thickness of the concrete cover will have a significant effect on preventing corrosive media from reaching the steel. In theory, the thicker the concrete cover of the structure, the longer the path for chloride ions to diffuse to the steel surface, thus slowing corrosion. However, the excessive thickness of the protective layer will limit the mechanical performance of the component, which can be detrimental to controlling the crack width.

3.4.2 Component form

Ensuring the compactness of concrete and thickness of the concrete cover in areas with significant component changes can be challenging. As a result, sites with substantial changes in component form will also experience severe corrosion.

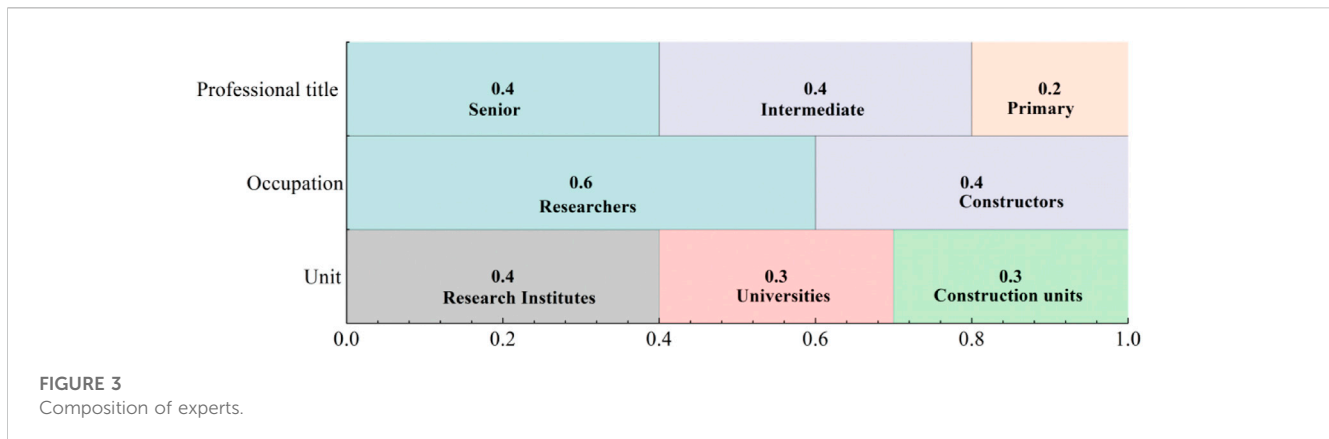
3.4.3 Construction quality

Structural quality factors such as concrete vibration, correct placement of steel, and concrete curing effect will directly determine the ability of concrete to resist erosion.

4 Establishment of an evaluation model

4.1 Identification of factors

The factors of chloride resistance could be identified by analyzing the influencing factors of chloride ion corrosion discussed in Section 3, combined with the expert survey results.



4.1.1 Expert selection

Experts participating in the survey were selected from research institutes, universities, and construction units to ensure that factor determination was scientific, authoritative, and reliable. Professional titles covered senior, intermediate, and primary, with senior and intermediate personnel having more engineering experience, accounting for 40% of the total. The occupation of experts included 60% researchers and 40% constructors, with constructors providing practical engineering experience. The total number of experts was 20, and the composition of experts is shown in Figure 3.

4.1.2 Analysis of factors

After considering chloride resistance from a theoretical perspective and the investigation results from experts, the factors that contributed to the chloride resistance of concrete were identified.

4.1.2.1 Concrete chlorine resistance

The chlorine resistance of concrete includes chloride ion permeability, chloride ions in raw materials, concrete mix design, and concrete covers.

(1) Chloride ion permeability (electric flux method or RCM method)

The electric flux method or RCM method has been mainly used to evaluate the chloride resistance of concrete according to Chinese codes. In this study, the evaluation of chloride ion permeability was based on the results of these methods.

According to the Code for Durability Design of Concrete Structures in Highway Engineering (JTG/T3310-2019) standard, for tidal and splash areas in hot areas (annual average temperature higher than 20°C), the environmental action level of concrete structures was found to be III-F. The limited D_{RCM} (28 days) should be $4 \times 10^{-12} \text{ m}^2/\text{s}$ with a design service life of 100 years, the limited D_{RCM} (28 days) should be $5 \times 10^{-12} \text{ m}^2/\text{s}$ with a design service life of 50 years, and the electric flux (56 days) should be limited to 800 C.

When applying concrete in the torrid marine region in China's Hainan Province, according to the technical standard for the application of ready-mixed concrete in Hainan Province (DBJ46-

18-019), the D_{RCM} (84 days) should be no more than $2.5 \times 10^{-12} \text{ m}^2/\text{s}$, or 56 days, and the electric flux should not exceed 1000 C.

The limit of chloride ion permeability in the RCM method could be identified by the engineering requirements and other standards and specifications related to engineering.

1) Limit of chloride ions in the raw materials

The Technical Code for the Application of Sea Sand Concrete (JGJ 206-2010) standard for water-soluble chloride ion content (cement mass percentage) of sea sand concrete mixture should be used when utilizing desalinated sea sand in civil engineering. When using plain concrete, the maximum content of water-soluble chloride ions should be 0.3%, and in humid and chloride-containing environments and corroded environments, the maximum content of water-soluble chloride ions in reinforced concrete should be 0.06%.

According to the Technical Standard for the Application of Ready-Mixed Concrete in Hainan province (DBJ46-18-019), the chloride ion content of sand is listed as a mandatory inspection item, when applying concrete in the torrid marine region in China's Hainan Province. The chloride ion content of sand for reinforced concrete should not exceed 0.02%, and the chloride ion content of sand for prestressed concrete should not exceed 0.01%.

The limit of chloride ions in raw materials could be identified in engineering requirements and other standards and specifications related to engineering.

2) Concrete mix design

Concrete mix design factors include the water-cement ratio, the use of mineral admixtures, sand ratio control, aggregate performance, and the use of admixtures.

With decreasing water-cement ratio, the compactness of concrete will be enhanced, which will improve chloride resistance. Concrete pores can be effectively filled with the rational use of different types of mineral admixtures, such as FA, mineral powder, SF, and other mineral admixtures, increasing the compactness of concrete and improving its chlorine resistance. By controlling the sand content, the porosity of concrete can be improved, the compactness of concrete can be enhanced, and the

chlorine resistance of concrete can be improved. By improving the aggregate particle size and shape, concrete cracks can be controlled, thus improving the chloride resistance of concrete. Adding admixtures can also effectively control the water-cement ratio, improve concrete performance and compactness, and enhance the chlorine resistance of the concrete.

3) Concrete cover

According to the standard for the Design of Concrete Structure Durability (GBT50476-2019), in the tidal range and splash zones in torrid marine regions, the minimum concrete cover range should be 55–70 mm with a designed service life of 100 years. In addition, the specific value must be selected according to the differences in component shape and concrete strength grade.

When applying concrete in the torrid marine region in China's Hainan Province, the minimum concrete cover should be 50 mm in the atmospheric zone, mild salt spray zone, and water level fluctuation zone, 70 mm in the splash zone or severe salt spray zone, and 40 mm in the underwater zone, according to the Technical standard for application of ready-mixed concrete in Hainan province (DBJ46-18-019).

The limit of concrete cover can be identified by engineering requirements and other standards and specifications related to engineering.

4.1.2.2 Location of concrete structure

The effects of biological attachment and microorganisms in seawater on the chloride resistance of concrete in tidal and splash zones were found to be different. Concrete in tidal and splash zones will be affected by microorganisms in seawater, but generally, biological attachment has shown to be mainly concentrated in tidal zones, with relatively few organisms in splash zones. In testing chloride ion content in concrete, the splash zone was found to be generally more significant than the tidal range zone. The attached organisms in the upper and lower layers of the tidal range were also found to differ. In general, the lower layer of the tidal range area will be covered with oysters, with the upper layer of the tidal range area containing fewer oysters, and most of the site occupied by barnacles. Consequently, the location of concrete should be considered an influencing factor. The location of concrete includes the tidal range zone and splash zone, with the tidal range divided into the lower layer of the tidal range zone and upper layer of the tidal range zone.

4.1.2.3 Impact of marine organisms on concrete

1 Influence of marine biological adhesion on concrete

The influence of marine biological adhesion on concrete mainly includes the effects of biological adhesion on surface coating cracking, the impact of biological adhesion on coating corrosion, and the impact of biological adhesion on concrete.

The impacts of biological adhesion on surface coating cracking include biological adhesion causing large-scale coating damage, which can reduce the protective effect on concrete.

The effects of biological adhesion on coating corrosion consist of the following. After biological death, the shell will be decomposed by

microorganisms, producing acidic substances that further corrode the coating and concrete.

The effects of biological adhesion on concrete include the formation of a dense biofilm (oyster shell) in the lower layer of the tidal zone, which will reduce the chloride ion content inside the concrete. The upper layer of the biofilm in tidal range areas generally exhibits a flocculent structure with insufficient density, and concrete structures under the biofilm are generally not dense, with the low density of concrete affecting its chlorine resistance performance. The surface of the concrete in the splash zone will generally not be covered with the biofilm generated by biological attachment, with chloride ion content being the highest 25 mm inside the concrete.

Therefore, considering the impact of biological adhesion on coatings and concrete, relevant tests or similar engineering comparisons must be conducted at the project's location, to determine the actual effect of biological adhesion on concrete and surface coatings in the project area. When evaluating the chlorine resistance of concrete in the splash zone, the impact of biological adhesion in the splash zone may be disregarded based on the actual needs of the project and expert opinions, due to the relatively small amount of biological adhesion in the splash zone. When comparing the importance of performance indicators, the importance of factors affecting biological adhesion in the splash zone may be reduced.

2 The impact of marine microorganisms on concrete

Metabolic biofilms produce biological sulfuric acid that corrode concrete at the gas-liquid interface, and microorganisms will be transformed into corrosive hydrogen sulfide or sulfuric acid substances by *Thiobacillus*, which can cause corrosion damage to tidal and splash areas. Once corrosive damage occurs, it will also affect the chlorine resistance of concrete.

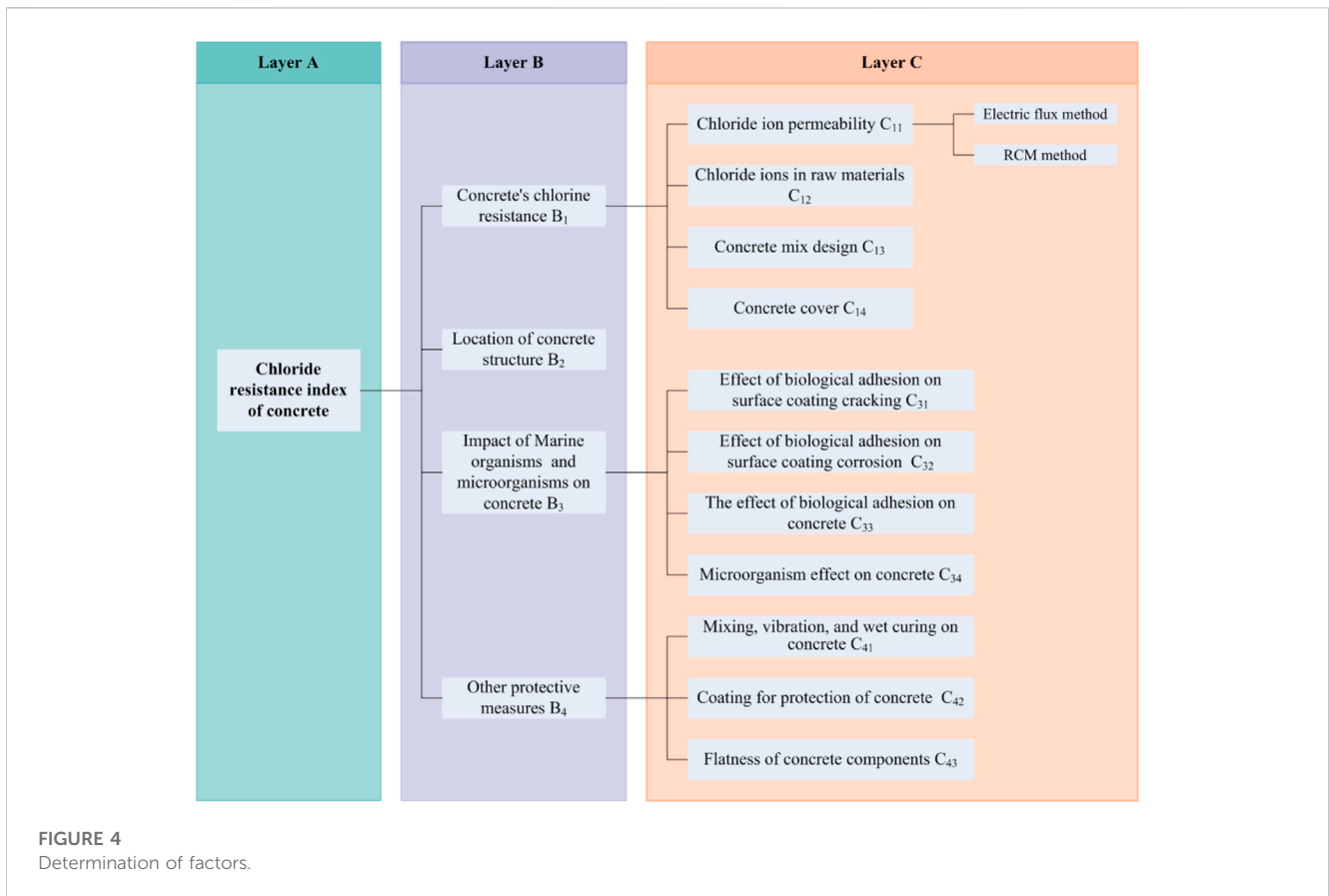
Microorganisms in different sea areas exhibit regional characteristics; thus, the degree of impact of marine microorganisms on concrete should be compared through relevant tests or similar projects in the project location to determine the actual degree of influence of marine microorganisms on concrete in the project location.

4.1.2.4 Other protective measures

The rationality and adequacy of mixing, vibration, and wet curing during the construction process will affect the compactness of concrete, thus affecting its chlorine resistance. The use of coatings to protect concrete during the construction process, such as epoxy resin coatings, polyurethane coatings, polyurea elastomer coatings, alanine latex coatings, and fluorine resin coatings, can reduce the penetration rate of Cl^- , CO_2 , and water, thus enhancing chlorine resistance. The flatness of the concrete component shape will affect the residual time of seawater on the components, thereby affecting the chlorine resistance of the concrete.

4.1.3 Factor determination

The characteristics and types of each factor can be used to classify the risk factors, with the assessment hierarchical structure illustrated in [Figure 4](#).



In terms of chloride ion permeability, the experiential method was used to select the electric flux method or RCM method, as shown in Figure 4.

4.2 Weight calculation

The weight of each factor could be calculated according to consistency certification. To ensure the scientificity, authority, and reliability of the judgment matrix results, experts were selected from different units to determine the value of a_{ij} in the judgment matrix. The composition of experts is shown in Figure 3, and the judgment matrix and weight calculations are presented in Table 6.

4.3 Membership function

Each factor could be divided into several levels, indicating that with the enhancement of grade, the chlorine resistance of marine concrete decreased. The division method was mainly based on statistical analysis, theoretical analysis, and experience. The purpose of partitioning was to facilitate the determination of membership.

According to regulatory requirements or engineering needs, the interval of membership functions could be partitioned. As shown in Table 7, the membership function could be divided into three levels.

The triangular fuzzy number could be defined based on the classification of factors, which was described by the numerical

method, with the triangular fuzzy number determined based on Table 7. The linguistic fuzzy number was defined according to the classification of factors, and the factor level was determined based on each element's category. Experts invited to the assessment could obtain fuzzy numbers found on the factor's level and the Karwowski fuzzy membership function, as shown in Table 4.

4.4 Estimation and results

The typical evaluation results were processed by the maximum value method, and the evaluation index corresponding to the maximum membership degree was taken as the assessment result. The chloride resistance was divided into three levels.

The maximum value method was used to describe the evaluation index corresponding to the maximum membership degree based on the calculation results, which served as the final evaluation result. According to the calculation, $B_i = \{B_1, B_2, B_3\}$ and $\max B_i = \max \{B_1, B_2, B_3\}$ were obtained.

Grade i corresponded to B_i , indicating the chloride resistance level of the concrete. Among these, B_1 grades indicated excellent chlorine resistance, B_2 indicated good chlorine resistance, and B_3 indicated average chlorine resistance.

When the measured values of any concrete chlorine resistance parameter did not meet the requirements of the specifications, it was directly determined that the concrete chlorine resistance was not qualified, and no further grading was conducted.

TABLE 6 Judgment matrix and weight calculations.

	B1	B2	B3	B4		c11	c12	c13	c14
B1	1	5	7	3	c11	1	1/3	3	7
B2	1/5	1	3	1/2	c12	3	1	9	9
B3	1/7	1/3	1	1/3	c13	1/3	1/9	1	3
B4	1/3	2	3	1	c14	1/7	1/9	1/3	1
$W = \{0.58, 0.13, 0.06, 0.22\}^T$, $\lambda_{\max} = 4.07$, $CI = 0.024$, $CR = 0.027 < 0.1$. Satisfying consistency					$W = \{0.25, 0.61, 0.09, 0.04\}^T$, $\lambda_{\max} = 4.13$ $CI = 0.042$, $CR = 0.047 < 0.1$. Satisfying consistency				
	c31	c32	c33	c34		c41	c42	c43	
c31	1	3	5	8	c41	1	1/3	4	
c32	1/3	1	2	3	c42	3	1	9	
c33	1/5	1/2	1	2	c43	1/4	1/9	1	
c34	1/8	1/3	1/2	1					
$W = \{0.25, 0.61, 0.09, 0.04\}^T$, $\lambda_{\max} = 4.13$					$W = \{0.60, 0.21, 0.12, 0.07\}^T$				
$CI = 0.042$, $CR = 0.047 < 0.1$ Satisfying consistency					$\lambda_{\max} = 4.01$, $CI = 0.04$, $CR = 0.04 < 0.1$ Satisfying consistency				

5 Application

The Hainan Province of China is located in the South China Sea region, with the characteristics of a torrid marine environment. Taking the Hainan Province project as an example, we evaluated the chlorine resistance of concrete in the tidal range and splash zone in torrid maritime regions and comprehensively proposed strategies for improving chlorine resistance.

5.1 Engineering overview

The Danzhou section of the Hainan Island Tour Highway, on which the project relies, has an average annual temperature of 23.5°C. The Danzhou region typically exhibits apparent characteristics of intense solar radiation, with this region exhibiting sufficient solar heat and an average yearly light duration of over 2000 h, the highest in the western coastal area, reaching around 2,500 h. Overall, Danzhou exhibits the apparent characteristics of a torrid marine environment.

The connection line of the Danzhou section project had a total length of 46.205 km, with 26 bridges arranged on the main line and most of the bridges in the project located in coastal sections. The area of the project location is shown in Figure 5A.

This project was supported by the Xiapu Bridge in the Danzhou section of the Hainan Island Ring Tourist Highway, with the Xiapu Bridge located at DZK64 + 862, crossing the Xiapu Port Discharge Lake, and the bridge site located 0.264 km away from the estuary. The tide typically has a high water level of 2.67 m once every 50 years, with the upstream portion of the bridge site located in a wetland with no prominent mainstream. The river has an upstream catchment area of 23.23 km², with the width of the channel at the investigated bridge site being about

105 m. The riverbed was relatively flat, with slow water flow. The water depth during the investigation was about 0.5 m (during ebb tide), and the bridge’s starting and ending points all consisted of shrublands, with steep slopes on both sides. The location of the Xiapu Bridge is shown in Figure 5B.

The compactness of the concrete of the Xiapu Bridge was improved by adding mineral admixtures and maintaining a low water-to-cement ratio. The actual mix proportion and technical conditions of piers columns in the project are shown in Table 8.

The mixing method, pouring time, and temperature of the formwork during the concrete construction process were strictly controlled.

The bridge’s pier body and cover beam were located in class III-D, III-E, and III-F environments, and the environmental action level was considered according to the severe salt spray area. The thickness of the protective layer was increased, and the concrete surface was treated. Furthermore, outer protective measures for the pier column involved applying two coats of primer (total film thickness 50 ± 10 mm), one coat of intermediate paint (total film thickness 300 ± 30 mm), and two coats of topcoat (total film thickness 100 ± 10 mm). The outer layer protection was achieved using a brush or roller or through spray coating.

The construction of the Xiapu Bridge is shown in Figures 5C,D.

5.2 Evaluation of concrete chlorine resistance

5.2.1 Basic information on influencing factors

According to the actual project conditions, the performance of marine concrete in some sections of the Hainan Island Ring Tourism Highway was selected as an engineering example for

TABLE 7 Classification of factors.

			Level 1	Level 2	Level 3
Chlorine resistance of the concrete	Chloride ion permeability	Electric flux method	$\frac{Q_s}{[Q_s]} < 0.25$	$0.25 \leq \frac{Q_s}{[Q_s]} < 0.5$	$0.5 \leq \frac{Q_s}{[Q_s]} \leq 1$
		RCM method	$\frac{D_{RCM}}{[D_{RCM}]} < 0.5$	$0.5 \leq \frac{D_{RCM}}{[D_{RCM}]} < 0.75$	$0.75 \leq \frac{D_{RCM}}{[D_{RCM}]} \leq 1$
	Limit of chloride ions in raw materials		$\frac{CF}{[CF]} < 0.5$	$0.5 \leq \frac{CF}{[CF]} < 0.75$	$0.75 \leq \frac{CF}{[CF]} \leq 1$
	Concrete mix design		Reasonable use of mineral admixtures and admixtures to effectively increase compactness	The use of mineral admixtures and admixtures increased the compactness	Mineral admixtures and admixtures were not used
	Concrete cover $c - [c]$ (mm)		$10 < c - [c]$	$5 < c - [c] \leq 10$	$0 < c - [c] \leq 5$
Location of the concrete structure			The lower layer of the tidal range zone	The upper layer of the tidal range zone	Splash zone
Impact of marine organisms on concrete	Effect of biological adhesion on surface coating cracking		Protect the coating	No effect on coating	Causing coating cracking
	Effect of biological adhesion on surface coating corrosion		Negligible corrosion of the coating	Coating corrosion	Severe deterioration of the coating
	Effect of biological adhesion on concrete		Biological shells will protect the concrete	The impact of biology on concrete can be ignored	Biological corrosion of concrete
	Microorganism effect on concrete		The influence of microorganisms on concrete can be ignored	Microbial corrosion of concrete	Microbial decomposition of concrete is severe
Other protective measures	Mixing, vibration, and wet curing on concrete		Reasonable mixing and vibration, with adequate wet curing	Mixing and vibration are more affordable	The rationality of mixing and vibration is average
				Wet curing is sufficient	The wet curing effect is average
	Coating for protection of concrete		The density, uniformity, and thickness of the coating meet the requirements	The coating's density, uniformity, and thickness meet the requirements relatively well	No coating for protection
	The flatness of concrete components		The components were flat and smooth, with no unevenness in shape	The components were flat and smooth, with concave and convex shapes	Insufficient flatness and smoothness of the components, with uneven shapes
			The components were relatively flat and smooth, with no concave or convex shapes		

analysis, and various index factors in the chlorine resistance of the concrete were graded. The membership function results were calculated by Karwowski's fuzzy membership function and the triangular membership function, where the different values in B_2 represented the use of concrete in the tidal and splash regions. In the application, the index of chloride ion permeability used the RCM method, as shown in Figure 6.

The RCM test used $\phi 100 \text{ mm} \pm 1 \text{ mm}$ diameter cylindrical specimen with a height of $50 \text{ mm} \pm 2 \text{ mm}$, and the maximum particle size of the aggregate in the sample did not exceed 25 mm. After specimen formation, they were immediately covered with plastic film and moved to a standard curing room. The specimens were then de-molded within $24 \text{ h} \pm 2 \text{ h}$ and immersed in a water tank in a standard curing room. The curing period of the specimens was 28 days, and other curing periods required for the test were also used.

5.2.2 Evaluation of chlorine iron resistance

The chloride resistance of concrete in the splash zone, the upper layer of the tidal range zone, and the lower layer of the tidal

range zone of the Xiapu Bridge was calculated. For the convenience of construction, the concrete mix design, raw materials, and construction quality control were among the different concrete structure factors. Therefore, the membership functions at different positions had the same values in the concrete chlorine resistance and other protective measure projects. According to the relationship between different concrete and marine organism positions, the membership function of each item in the impact of marine organizations on concrete was selected. The evaluation results of the chlorine resistance of Pier 6 in the Xiapu Bridge were obtained through calculation, and the results are shown in Table 9.

According to the evaluation results of the chlorine resistance of Pier 6 in the Xiapu Bridge, we concluded that the chlorine resistance in both tidal and splash zones could reach a good level. The evaluation calculation results showed that the probability of the upper layer concrete chlorine resistance was good in the tidal zone, and this was more significant than that in the splash zone. The likelihood that the upper layer chlorine resistance of the concrete was average in the tidal area was half that in the splash zone. Therefore, although the same design and construction methods were

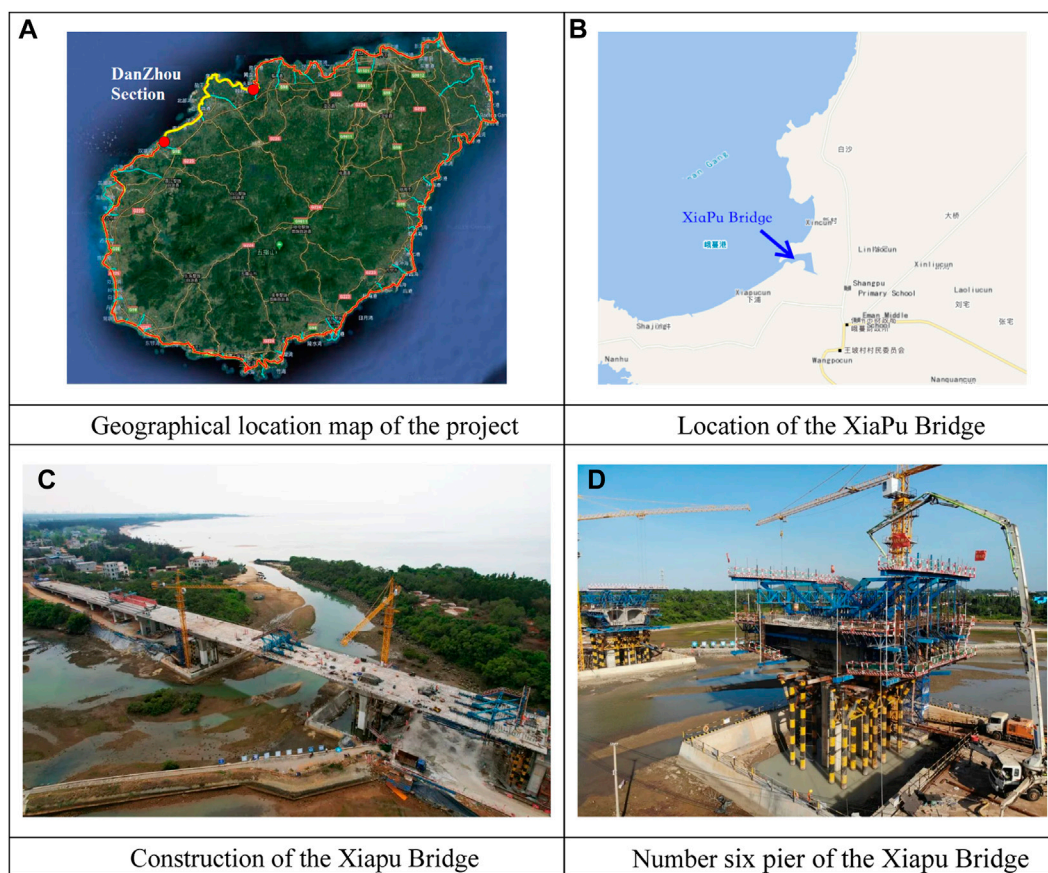


FIGURE 5 Location and construction of the project. (A) Geographical location map of the project. (B) Location of the XiaPu Bridge. (C) Construction of the XiaPu Bridge. (D) Number six pier of the XiaPu Bridge.

TABLE 8 Concrete mix ratio in pier columns.

	Cement PO42.5	Grade I fly ash	S95 slag powder	Fine aggregate (medium sand)	Coarse aggregate	Polycarboxylate high-performance water reducer	Rust remover	Water
Mix proportion	1	0.21	0.21	2.19	3.74	0.016	0.10	0.4
Amount kg/m ³	308	66	66	676	1,150	4.84	30	124
Water-to-cement ratio	Percentage of sand (%)	Measured slump (mm)	Apparent density (kg/m ³)	Compressive strength (7 days)	Compressive strength (28 days)	$D_{RCM} \times 10^{-12} \text{ m}^2/\text{s}$		
				(MPa)	(MPa)			
0.35	37	195	2,430	45.8	54.1	4.7		

used, the chlorine resistance of the upper layer of concrete in the tidal zone was still better than that in the splash zone. The possibility that the chloride resistance of the concrete in the lower layer of the tidal range zone was excellent, and it was significantly higher than in the upper layer and splash zone of the tidal range zone. In addition, from a numerical perspective, the chlorine resistance of the upper layer in the tidal range area was close to the excellent level.

Therefore, to improve the overall chlorine resistance of Pier 6 in the Xiapu Bridge, more methods could be used to further enhance the

chlorine resistance of the concrete in the upper layer of the splash zone and tidal range zone.

5.3 Measures to improve the chlorine resistance of concrete in torrid marine regions

The reasonable design of concrete component structural systems, as well as the adoption of suitable structural measures, serves as an

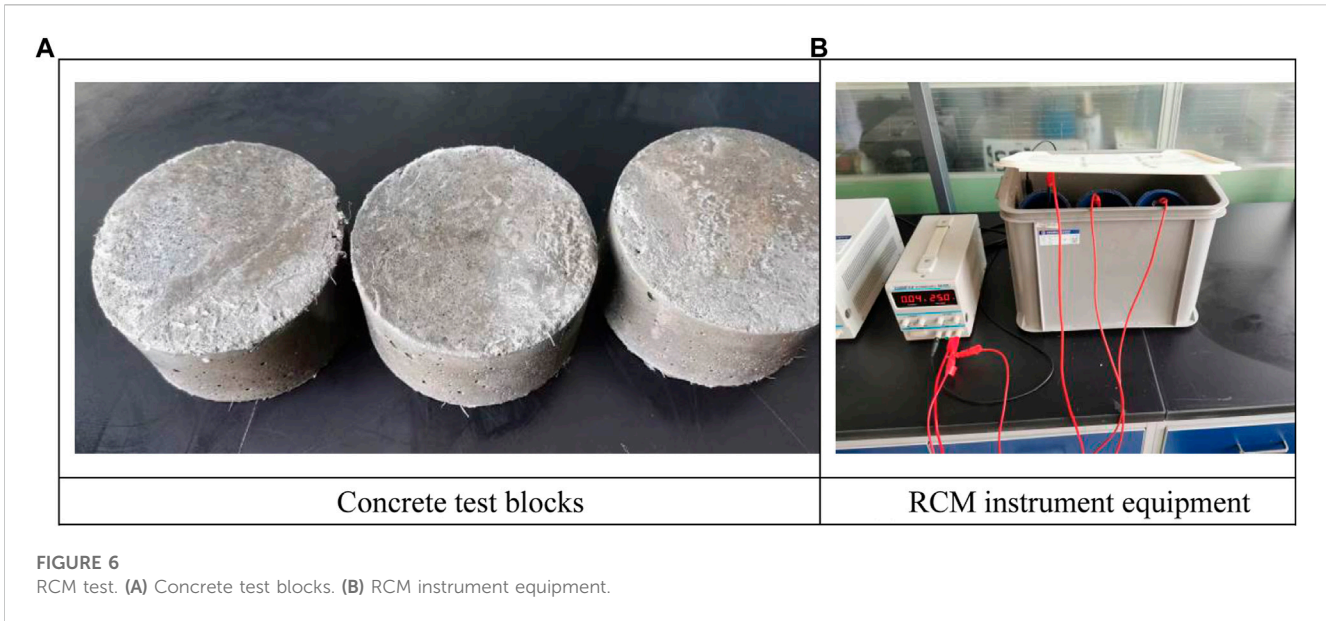


FIGURE 6
RCM test. (A) Concrete test blocks. (B) RCM instrument equipment.

TABLE 9 Chlorine resistance of Pier 6 of Xiapu Bridge.

Location of the concrete structure	Fuzzy estimation results of chlorine resistance			Chlorine resistance			Evaluation level
				Excellent	Good	Average	
Splash zone	0.35	0.49	0.16	0.35	0.49	0.16	Good
The upper layer of the tidal range zone	0.35	0.57	0.08	0.35	0.57	0.08	Good
The lower layer of the tidal range zone	0.45	0.49	0.06	0.45	0.49	0.06	Good

important influencing factor for the corrosion prevention of concrete structures. The specific criteria for improving chlorine resistance could be summarized as follows:

1. For concrete in torrid marine regions, based on acceptable design, the span of the bridge should be increased, while the number of substructure structures should be reduced. Therefore, substructure structures in the tidal range and splash areas should be minimized where corrosion is most severe.
2. Each bridge component’s appearance, structural cross-section, and detailed structure should be designed as smooth, continuous, and simple as possible to avoid sudden changes, stress concentrations, and cracking of the structural components. In addition, water accumulation must be prevented in parts with insufficient compactness of the construction concrete, inadequate thickness of the concrete cover, and improper placement of the steel bars.
3. Design changes or protective measures should be made to components prone to corrosion.
4. According to marine corrosion conditions and the characteristics of structural components, the concrete cover should be appropriately increased.

6 Conclusion

Based on China’s long-term goals for 2035, many projects are expected to be constructed in **torrid** marine regions, and

concrete engineering in tidal and splash zones in these regions will be more susceptible to chloride ion erosion. Consequently, it is critical to assess the chloride resistance of concrete in the tidal range and splash zones in torrid marine regions. The enhanced F-AHP method was applied in this study, where various influencing factors with tropical marine environmental characteristics were considered, including the impact of marine organisms on concrete and the differences in chloride resistance in tidal and splash zones. These have not been assessed in previous chlorine resistance studies.

- (1) The factors affecting the chloride resistance of concrete in the tidal range and splash zone in torrid marine regions were theoretically analyzed. Analysis mainly consisted of concrete material properties and marine environments, as well as external protection, design, and construction.
- (2) Factors were determined and classified according to concrete chlorine resistance, concrete structure location, and marine organism impact on concrete. These have not been frequently mentioned in previous chlorine resistance assessments and other protective measures, with the factors containing experimental results, theoretical basis, and engineering conditions. The weight of each element was calculated in the enhanced F-AHP method to ensure the consistency of judgment matrices from expert investigations. Membership functions were obtained based on engineering requirements, standards, and specifications related to the project to enhance its applicability to engineering, and

the assessment results were classified into three levels to measure chlorine resistance.

- (3) Assessment was applied to marine concrete engineering in the tidal range and splash zones for the Xiapu Bridge in Hainan Province, China, with apparent characteristics of a torrid marine environment. Methods for improving the chlorine resistance of concrete were proposed according to the project and assessment factors.
- (4) An assessment was constructed to estimate the chlorine resistance of concrete in torrid marine regions. The sulfate content in these areas was higher than that in other marine areas, indicating that the assessment of sulfate resistance in concrete in the tidal range and splash zones of torrid marine regions should be studied in the future. In this assessment, the impact of marine organisms and microorganisms on concrete was based on expert surveys. Because of qualitative description factors, the impact of marine organisms and microorganisms on concrete may be quantified in the future, and the membership function will be updated.

Data availability statement

The raw data supporting the conclusion of this article will be made available by the authors, without undue reservation.

Author contributions

YY: Conceptualization, Formal Analysis, Investigation, Methodology, Writing—original draft. NC: Conceptualization,

Writing—review and editing. LL: Validation, Writing—review and editing. JW: Validation, Writing—review and editing.

Funding

The author(s) declare financial support was received for the research, authorship, and/or publication of this article. This research was funded by the PILOT PROJECT OF RIOH FOR A COUNTRY WITH STRONG TRANSPORTATION NETWORK-3.2 Research and development, promotion and application of safety and durability technology for highway bridges, grant number 2021-1-3-2.

Conflict of interest

Author YY, NC, and LL are employed by the Research Institute of Highway Ministry of Transport. Author JW is employed by the China Highway Engineering Consulting Corporation.

Publisher's note

All claims expressed in this article are solely those of the authors and do not necessarily represent those of their affiliated organizations, or those of the publisher, the editors and the reviewers. Any product that may be evaluated in this article, or claim that may be made by its manufacturer, is not guaranteed or endorsed by the publisher.

References

- Al-Hashem, M. N., Amin, M. N., Ajwad, A., Afzal, M., Khan, K., Faraz, M. I., et al. (2022). Mechanical and durability evaluation of metakaolin as cement replacement material in concrete. *Materials* 15, 7868. doi:10.3390/ma15227868
- Amin, M. N., Raheel, M., Iqbal, M., Khan, K., Qadir, M. G., Jalal, F. E., et al. (2022). Prediction of rapid chloride penetration resistance to assess the influence of affecting variables on metakaolin-based concrete using gene expression programming. *Materials* 15, 6959. doi:10.3390/ma15196959
- Bastidas-Arteaga, E., Schoefs, F., Chateaufneuf, A., Sánchez-Silva, M., and Capra, B. (2010). Probabilistic evaluation of the sustainability of maintenance strategies for RC structures exposed to chloride ingress. *Int. J. Eng. Uncertain. Hazards Assess. Mitig.* 2, 61–74.
- Cai, J. G., Dong, F. H., and Luo, Z. L. "Durability of concrete bridge structure under marine environment." *J. Coast. Res.*, vol. 83, no. sp1, pp. 429–435. doi:10.2112/si83-072.12019
- Chen, J., Bao, X. Y., and Zhao, Y. L. (2015). On the assessment of the durability of the concrete bridges in service via the fuzzy EAHP. *J. Saf. Environ.* 15 (4), 16–20. doi:10.13637/j.issn.1009-6094.2015.04.003
- Habib, M., Saad, M., and Abbas, N. (2022). Evaluation of mechanical and durability aspects of self-compacting concrete by using thermo-mechanical activation of bentonite. *Eng. Proc.* 22, 17. doi:10.3390/engproc202202017
- Huang, X., Wang, S., Lu, T., Li, H., Wu, K., and Deng, W. (2023). Chloride permeability coefficient prediction of rubber concrete based on the improved machine learning technical: modelling and performance evaluation. *Polymers* 15, 308. doi:10.3390/polym15020308
- Imounga, H. M., Bastidas-Arteaga, E., Moutou Pitti, R., Ekomy Ango, S., and Wang, X.-H. (2020). Bayesian assessment of the effects of cyclic loads on the chloride ingress process into reinforced concrete. *Appl. Sci.* 10, 2040. doi:10.3390/app10062040
- Karwowski, W., and Mital, A. (1986). Applications of approximate reasoning in risk analysis - ScienceDirect. *Adv. Hum. Factors/Ergonomics* 6, 227–243. doi:10.1016/B978-0-444-42723-6.50020-9
- Lee, J., and Lee, T. (2020). Durability and engineering performance evaluation of CaO content and ratio of binary blended concrete containing ground granulated blast-furnace slag. *Appl. Sci.* 10, 2504. doi:10.3390/app10072504
- Lee, J., Lee, T., Choi, H., and Lee, D.-E. (2020). Assessment of optimum CaO content range for high volume F.A. Based concrete considering durability properties. *Appl. Sci.* 10, 6944. doi:10.3390/app10196944
- Li, F., Phoon, K. K., Du, X., and Zhang, M. (2013). Improved AHP method and its application in risk identification. *J. Constr. Eng. Manag.* 139, 312–320. doi:10.1061/(asce)co.1943-7862.0000605
- Li, T., Huang, Y. E., and Xiang, J. (2021). Durability evaluations of sea-spanning tied-arch bridges based on fuzzy extensive sets. *J. Central South Univ.* 52 (7), 2470–2479. doi:10.11817/j.issn.1672-7207.2021.07.032
- Luhar, S., Luhar, I., Nicolaidis, D., and Gupta, R. (2021). Durability performance evaluation of rubberized geopolymer concrete. *Sustainability* 13, 5969. doi:10.3390/su13115969
- Lyu, H.-M., Sun, W.-J., Shen, S.-L., and Zhou, A.-N. (2020). Risk assessment using a new consulting process in fuzzy AHP. *J. Constr. Eng. Manag.* 146. doi:10.1061/(asce)co.1943-7862.0001757
- Mathews, M. E., Kiran, T., Nammalvar, A., Anbarasu, M., Kanagaraj, B., and Andrushia, D. (2023). Evaluation of the rheological and durability performance of sustainable self-compacting concrete. *Sustainability* 15, 4212. doi:10.3390/su15054212
- Mehta, P. K. (1997). Durability—critical issues for the future. *Concr. Int.* 19, 27–33.
- Melchers, R. E., and Chaves, I. A. (2021). Durable steel-reinforced concrete structures for marine environments. *Sustainability* 13, 13695. doi:10.3390/su132413695
- Mukhti, J. A., Robles, K. P. V., Lee, K.-H., and Kee, S.-H. (2023). Evaluation of early concrete damage caused by chloride-induced steel corrosion using a deep learning approach based on RNN for ultrasonic pulse waves. *Materials* 16, 3502. doi:10.3390/ma16093502
- Poupard, O., L'Hostis, V., Catinaud, S., and Petre-Lazar, I. (2006). Corrosion damage diagnosis of a reinforced concrete beam after 40 years natural exposure in marine environment. *Cem. Concr. Res.* 36, 504–520. doi:10.1016/j.cemconres.2005.11.004
- Prithiviraj, C., Saravanan, J., Ramesh Kumar, D., Murali, G., Vatin, N. I., and Swaminathan, P. (2022). Assessment of strength and durability properties of self-

- compacting concrete comprising alccofine. *Sustainability* 14, 5895. doi:10.3390/su14105895
- Richardson, M. G. (2002). *Fundamentals of durable reinforced concrete*. London, UK: Spon Press.
- Rong, H., Cheng, X. J., Liu, D. E., Zhang, Y., Zhang, L., Feng, Y., et al. (2021). Research progress on macro biological corrosion of marine concrete. *J. Chin. Ceram. Soc.* 50, 503–511. doi:10.14062/j.issn.0454-5648.20210719
- Saaty, T. L. (1980). *The analytic hierarchy process*. New York: McGraw Hill.
- Saaty, T. L. (2001). *Encyclopedia of operations research and management science*. New York: Springer US. Analytic hierarchy process
- Stratoura, M. C., Lazari, G.-E. D., Badogiannis, E. G., and Papadakis, V. G. (2023). Perlite and rice husk ash Re-use as fine aggregates in lightweight aggregate structural concrete—durability assessment. *Sustainability* 15, 4217. doi:10.3390/su15054217
- Wang, J. C., and Yan, P. Y. (2009). There search of the corrosion mechanism of the marine bio-fouling to the concrete. *Concr.* 10, 7. doi:10.3969/j.issn.1002-3550.2009.10.007
- Wang, J., and Yan, P. (2009). Literature review of corrosion mechanism of marine fouling organisms on concrete. *Concrete* 240 (10), 24–26. doi:10.3969/j.issn.1002-3550.2009.10.007
- Yennawar, P. L., Thakur, N. L., Anil, A. C., Venkat, K., and Wagh, A. Ecology of the wood-boring bivalve *martesia striata*(pholadidae) in Indian waters[J].*Estuar. Coast. Shelf Sci.*,1999,48(A):123–130. doi:10.1016/S0272-7714(99)80017-1
- Yoon, C. B., and Lee, H. S. (2020). Selection of the optimum carrier for manufacturing water-repellent concrete and durability evaluation of cement mortar using it. *Appl. Sci.* 10, 9097. doi:10.3390/app10249097
- Yu, Y., He, X., Wan, F., Bai, Z., and Fu, C. (2022). Dynamic risk assessment of karst tunnel collapse based on fuzzy-AHP: a case study of the LianHuaShan tunnel, China. *Adv. Civ. Eng.* 2022, 1–17. doi:10.1155/2022/4426318
- Yuan, T.-F., Hong, S.-H., Choi, J.-S., and Yoon, Y.-S. (2021). Evaluation on the microstructure and durability of high-strength concrete containing electric arc furnace oxidizing slag. *Materials* 14, 1304. doi:10.3390/ma14051304
- Zadeh, L. A. (1965). Fuzzy sets. *Inf. Control* 8 (3), 338–353. doi:10.1016/s0019-9958(65)90241-x